

Adaptive estimation of the transformer stray capacitances for DC–DC converter modelling

ISSN 1755-4535

Received on 3rd February 2016

Revised on 12th August 2016

Accepted on 18th August 2016

doi: 10.1049/iet-pel.2016.0053

www.ietdl.org

Piotr Musznicki ✉, Piotr J. Chrzan, Marcin Rucinski, Maciej Kolincio

Faculty of Electrical and Control Engineering, Gdańsk University of Technology, G. Narutowicza 11/12, 80-233 Gdańsk, Poland

✉ E-mail: piotr.musznicki@pg.gda.pl

Abstract: New low cost and accurate estimation method of transformer stray capacitances for wide band DC–DC converter modelling and design is proposed. The Wiener filter (WF) method is applied to estimate the transformer impedance – referred to the selected transformer winding configurations. Laboratory tests are used to adapt the filter, that is to find optimal impedance which minimises mean square error between measured, noise perturbed current and reconstructed current. Transformer transfer function peaks indicate internal LC resonances. Stray capacitances are extracted based on resonant frequencies determination. The method validation is carried out by simulation and experimental analysis, where estimated stray capacitances by WF are compared with measurements of an impedance analyser.

1 Introduction

Requirements and fulfilment of EMC standards in early stage of DC–DC converters design process, need wide band modelling and simulation environment. The simulation circuits should contain models of lumped components including basic and parasitic parts. Such models take into account all phenomena encountered in the frequency range of conducted emissions up to 30 MHz. The DC–DC converter high frequency transformer parameters, such as leakage inductance and stray capacitances are of special concern for prediction of the EMI emissions or ringing frequencies for snubber dimensioning [1, 2]. Moreover they can be used as resonant elements in soft-switched DC–DC converters [3]. The selection of the optimal transformer to fulfil the electromagnetic compatibility standards requires information about the leakage inductance and parasitic capacitance [4, 5]. In producer datasheets, the leakage inductance is principally specified, however the stray capacitances are usually neglected, being more dependent on circuit modelling assumptions.

Much effort has been given in literature to the transformer parameters extraction. Geometrical dimension and electromagnetic models using finite element analysis have been applied to calculate parasitic capacitances [6–9]. These methods require precise knowledge about winding geometry and can give inaccurate results due to random wires replacement during production. Moreover, they are time and calculation power consuming.

Experimental setup for the two-port network approach using the step response [10, 11] and the frequency response analysis [12–14] have been presented. Non-linear identification process, taking into account magnetic saturation and skin effects occurring in the windings, have been described in [15]. Application of these methods requires specialised measurement setups and may be burdened for small and medium power devices by additional parasitic capacitances of measuring circuits. Bayesian approach for estimation of transformer parameters has been applied in [16], however without modelling of winding distributed capacitances and the primary–secondary interwinding capacitance.

In this paper a new method of the transformer stray capacitances adaptive estimation using digital signal processing procedure based on the Wiener filtering (WF) [17, 18] is presented. Due to the WF adaptation, circuit lumped parameters of the transformer are extracted, apart from other parasitic components of measurement equipment, as e.g. power supplies and wires, that are not included into estimated transfer function. The main advantage of this estimation is high speed, accuracy and low cost.

2 Modelling and estimation

The high frequency transformer lumped circuit model is assumed as in Fig. 1 [19]. It consists of the magnetising inductance, which is referred to the primary L_{M1} transformer circuits with primary and secondary leakage inductances $L_{\sigma 1} = n^2 L_{\sigma 2}$ (n -turns ratio), winding resistances R_1, R_2 , primary C_1 and secondary C_2 winding capacitances. The primary and secondary inter-winding capacitance is represented by capacitor C_{12} .

The transformer inductances and winding resistances can be directly determined by impedance bridge measurements. The stray capacitances estimation needs a special treatment due to its relatively low value and interactions with other parasitic capacitances from the measurement equipment. In the conducted EMI frequency range, the impedance $Z(f)$ contains number of peaks which are connected with internal transformer resonant frequencies [20]. For the parasitic extraction, these resonant frequencies should be identified. The objectives of the present study are as follows:

- identification of transformer resonant frequencies using data from voltage and current measurements for each pair of transformer terminals based on WF [18],
- estimation of transformer capacitances using identified frequencies and measured inductances.

To find the WF transfer function, the voltage signal is used as excitation signal and the current is compared with filter output. After adaptation process the WF transfer function is an approximation of the transformer impedance. The analysis of the WF envelope transfer function spectra allows to identify the resonant frequencies which are used to estimate parasitic capacitance referred to primary side for the three transformer winding setups. Next, value of the equivalent lumped capacitances as in Fig. 1 are calculated.

3 Estimation method

To obtain the value of parasitic capacitances presented in Fig. 1, four steps are performed as presented in Fig. 2. First, the current and the voltage waveforms should be registered for three measurement setups, where the rectangular voltage waveform is used as the an excitation function for step response analysis. Second, measurement waveforms are used to adapt the WF, where its

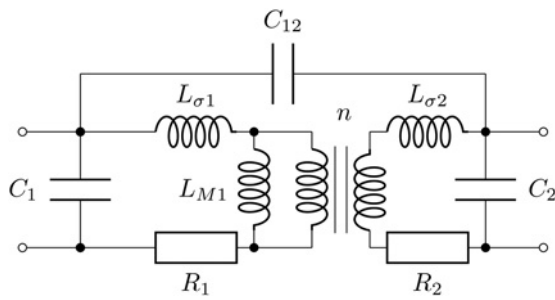


Fig. 1 Two winding transformer with stray capacitances effect

transfer function results from the transformer impedance. Third, dominant resonant frequencies – as depicted in Table 1 – are used to calculate equivalent capacitances C_{M1} , C_{M2} and C_{M3} . In the last step the estimated stray capacitances are derived.

4 Measurement setups

Parasitic capacitances, of the transformer, are associated with resonant frequencies, which can be observed in impedance spectra. The origin of these phenomena is interaction between inductances and capacitances of different transformer sides, layers, wires and other parts. The first lowest resonant frequency represents resonants between transformer inductance and the lumped equivalent capacitance. The equivalent model presented in Fig. 1 contains three lumped capacitances representing primary side winding self-capacitance C_1 , secondary side winding self-capacitance C_2 and capacitance between two windings C_{12} . These lumped capacitances can be estimated by analysing impedance spectra of three setup circuits [21]:

- with open secondary side (Fig. 3a),
- short circuit between primary winding end and secondary winding beginning (Fig. 3b),
- shorted secondary side terminals (Fig. 3c).

The setup circuits contain in addition to the transformer also voltage rectangular wave pulse generator V_{sq} with $50\ \Omega$ output,

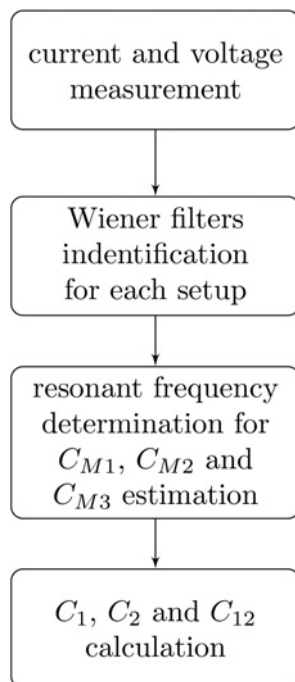


Fig. 2 Procedure of the transformer lumped capacitances extraction

Table 1 Equivalent input capacitances

	f [MHz]	$C = \frac{1}{(2\pi f)^2 L}$ [pF]
C_{M1}	3.27	51.13
C_{M2}	2.44	92.09
C_{M3}	14.6	49.5

high frequency current and voltage probes connected with oscilloscope. For proper results, the voltage impulses should be generated with appropriately short rising and falling times. The measured voltage and current waveforms are used to compute impedance using WF method described in Section 5.

4.1 C_{M1} measurement

The equivalent capacitance seen from primary winding terminals C_{M1} can be estimated using circuit presented in Fig. 3a, where secondary winding terminals are open. Assuming model from Fig. 1, it can be noted that C_{M1} is a parallel connection of C_1 and C_2 referred to the primary side. The equivalent input capacitance C_{M1} is given by the following formula

$$C_{M1} \simeq C_1 + \frac{C_2}{n^2} \quad (1)$$

4.2 C_{M2} measurement

In Fig. 3b is the short connection between primary winding end and secondary winding beginning. The first resonant frequency results from interaction between input inductance $L_0 = L_{M1} + L_{\sigma1}$ and capacitance C_{M2} , which is parallel connection of C_1 , C_{12} and C_2 referred to the primary side. The equivalent input capacitance C_{M2} is given by formula 2:

$$C_{M2} \simeq C_1 + C_{12} + \frac{C_2}{n^2} \quad (2)$$

4.3 C_{M3} measurement

In Fig. 3c the short circuit is between the terminals of secondary winding. It allows to oust the capacitances C_2 and C_{12} from impedance. The main resonant frequency results from interaction between C_1 and $L_{\sigma1}$.

The equivalent input capacitance C_{M3} is given by the following formula

$$C_{M3} \simeq C_1 \quad (3)$$

The capacitances C_{M1} , C_{M2} and C_{M3} can be derived using identified resonant frequencies by WF method.

$$C_{M1} = [L_0 \times (f_1 \times 2 \times \pi)^2]^{-1} \quad (4)$$

$$C_{M2} = [L_0 \times (f_2 \times 2 \times \pi)^2]^{-1} \quad (5)$$

$$C_{M3} = [2 \times L_{\sigma1} \times (f_3 \times 2 \times \pi)^2]^{-1} \quad (6)$$

where:

- f_1, f_2, f_3 are frequencies obtained from WF transfer function for distinctive resonances,
- $L_0 = L_{M1} + L_{\sigma1}$ input inductance,

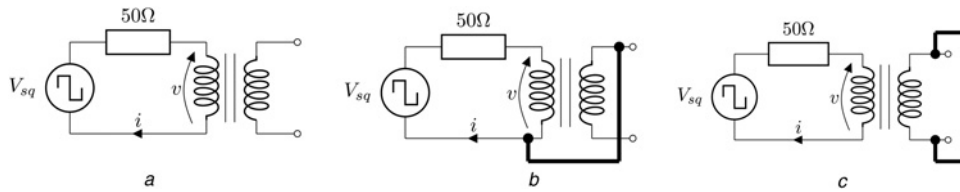


Fig. 3 C_{M1} , C_{M2} and C_{M3} measurement setups

- $2 \times L_{\sigma 1} \approx L_{\sigma 1} + n^2 \times L_{\sigma 2}$ sum of leakage primary and secondary inductances.

Based on (4), (5) and (6), capacitances of the transformer model (Fig. 1) are calculated.

$$C_1 = C_{M3} \quad (7)$$

$$C_2 = n^2 \times (C_{M1} - C_{M3}) \quad (8)$$

$$C_{12} = C_{M2} - C_{M1} \quad (9)$$

5 Transfer function identification using WF

The WF method can be applied to estimate the transfer function between two signals corrupted with additive noise [17, 18]. Thus, using measurement results, as described in Section 4, the transformer impedances are obtained. In this case, the input signal is the rectangular wave voltage v excitation across transformer terminals and the output is the current i measured with additive noise. Block diagram representing WF applied to transformer impedances estimation by adapted filter H is depicted in Fig. 4.

All signals are expressed in the frequency domain using the Fourier transformation of the voltage v , noted $V(j\omega)$ and current i , noted $I(j\omega)$. To reduce the noise (coming from other sources, numerical and sampling resolution), averaging procedure is employed. The aim of adaptation process is to find the optimal value of the frequency response which minimises mean square error $E_r(j\omega)$ between measured and reconstructed current signals.

$$E_r(j\omega) = I(j\omega) - I_r(j\omega) = I(j\omega) - H(j\omega)V(j\omega) \quad (10)$$

The mean square error between measured and reconstructed current can now be defined in the frequency domain as:

$$E[|E_r(j\omega)|^2] = E[(I(j\omega) - H(j\omega)V(j\omega)) * (I(j\omega) - H(j\omega)V(j\omega))] \quad (11)$$

where $E[\cdot]$ denotes the expectation operator and $*$ the complex conjugate.

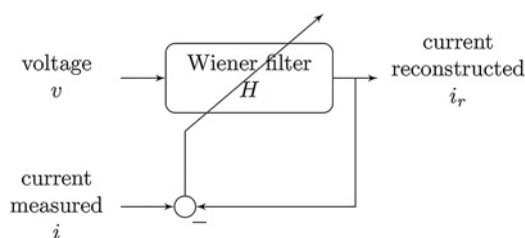


Fig. 4 WF applied to impedance measurement

To minimise this error, the derivative of complex quadratic form (11) with respect to $H(j\omega)$ has unique minimum, that yields

$$\frac{\partial E[|E_r(j\omega)|^2]}{\partial H(j\omega)} = 2H(j\omega)S_{vv}(j\omega) - 2S_{vi}(j\omega) = 0, \quad (12)$$

where:

- $S_{vv}(j\omega) = E[|V(j\omega)|^2]$ is the power spectrum of v ,
- $S_{vi}(j\omega) = E[V(j\omega)I^*(j\omega)]$ is the cross spectrum between v and i ,

From (12), the optimal transfer function $H_o(j\omega)$ expression in the frequency domain is given by:

$$H_o(j\omega) = \frac{S_{vi}(j\omega)}{S_{vv}(j\omega)}. \quad (13)$$

6 Method validation based on simulation results

To verify the capacitance estimation method, simulation model has been examined. Simulation was performed for the circuit presented in Fig. 5a using *Saber@Sketch* simulator. The scheme has been constructed as hierarchical model, where transformer circuit is presented in Fig. 5b.

The parameter values were typical for transformer used in a low power (≤ 300 W) DC-DC converter.: $C_1 = 50$ pF, $C_2 = 15$ pF, $C_{12} = 40$ pF, primary side leakage inductance $L_{\sigma} = 1.2$ μ H and magnetising inductance $L_{M1} = 45$ μ H. The voltage source connected to primary side of transformer is rectangular wave generator (piecewise linear voltage source model) operating with frequency $f_G = 100$ kHz and rise/fall time $t_r = 1$ ns. The sampling frequency (nominal calculation step) was set at 0.1 ns for transient simulation.

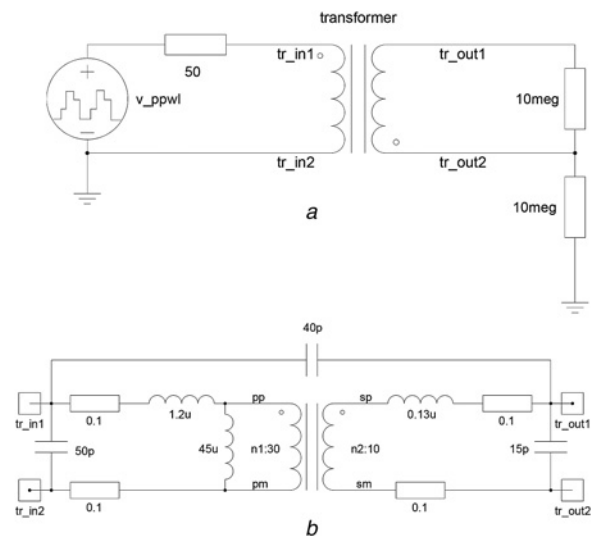


Fig. 5 Simulation circuit in the *Saber@Sketch*

a Test circuit

b Transformer model

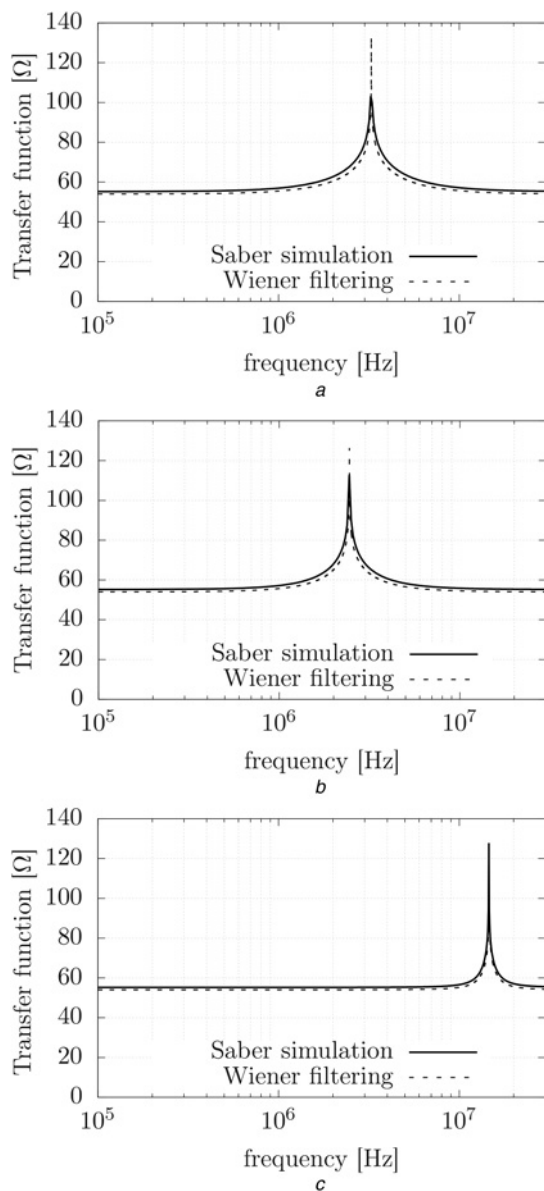


Fig. 6 Transfer function from Saber simulation and WF for circuit from Fig. 3

To verify method, the AC sweep analysis was done, where voltage source was characterised by variable frequency source. The voltage of transformer primary terminals and input current were used to calculate impedance in the frequency domain (Fig. 6). Equivalent input capacitances derived from (4)–(6) and impedance resonant frequencies are given in Table 1.

The simulation results of the three configurations (Figs. 3a–c), were used for impedance computation carried out in Saber@ and to determine WF transfer functions using Matlab@ software (Fig. 6).

The transformer stray capacitances are then calculated directly from (7)–(9). Results and comparison with simulation model parameters are presented in Table 2.

The estimated parameters have comparative values with simulated in Saber@ model, which validates method.

Table 2 Stray capacitances resulting from the simulation model impedance and the WF estimation

	C_{model} [pF]	C_{WF} [pF]	error %
C_1	50	49.5	0.9
C_{12}	40	40.8	2
C_2	15	15.8	5



Fig. 7 Transformer used in experimental tests

7 Example of measurement

The estimation of capacitance was evaluated for self-made laboratory transformer (Fig. 7). Magnetising inductance, leakage inductance and stray capacitances has been measured with the impedance analyser KEYSIGHT E4990A for three transformer setups (Table 3). The generator RIGOL DG4104 was used as rectangular voltage waveform source. The voltage and current were registered with the oscilloscope Textronix DP0 2012B with differential voltage probe (up to 100 MHz) and high frequency current probe (up to 50 MHz). Next, registered signals were used to adapt WFs for setups presented in Figs. 3a–c. Equivalent stray capacitance estimation carried out by the impedance analyser and transfer functions of WFs for these three setups are presented in Figs. 8, 9 and 10. The differences between impedance characteristics result from measurement conditions. Using WF method we apply voltage signal generator with its internal 50 Ω resistance connected in series with the measured transformer setup. Thus, the damping factor of the first dominant resonant circuit is much increased with respect to the impedance analyser measurement circuitry. Moreover, in the proposed WF method we apply constant frequency rectangular waveform excitation, while an impedance analyser scans the circuit with variable frequency sinusoidal excitation. Nevertheless, both methods provide similar stray capacitance values (Table 4).

In real transformer – in contrary to simulation model – more resonant frequencies appear, because of distributed capacitances effect. The dominant frequency peaks for setups presented in Figs. 8–10 have been taken into consideration and they appear for

Table 3 Transformer parameters

Parameter	Value
core shape	PM
core material	N27 from EPCOS
output–input ratio	0.286
magnetising inductance	120.8 μH
primary leakage inductance	6.13 μH
primary winding resistance	85 mΩ
secondary winding resistance	114 mΩ

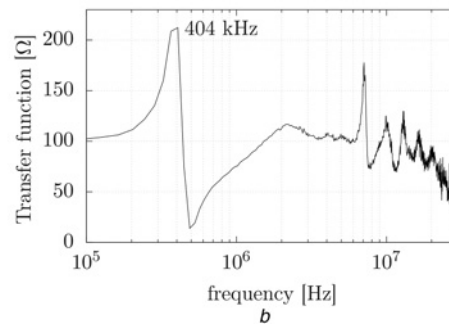
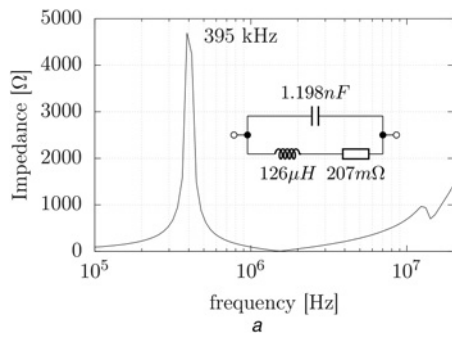


Fig. 8 C_{M1} measurement with
 a Impedance analyser
 b WF transfer function

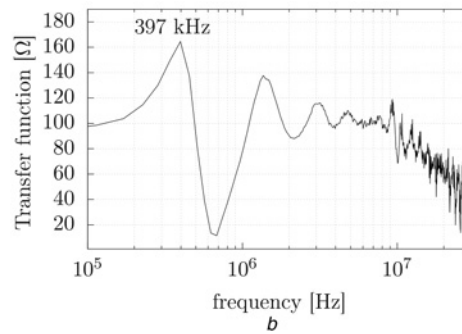
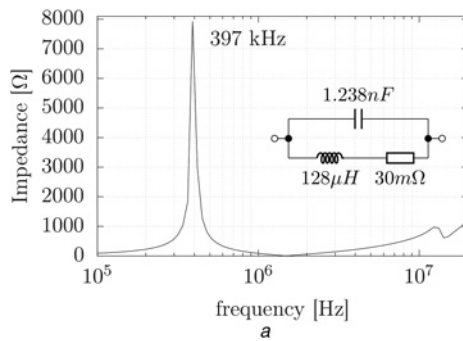


Fig. 9 C_{M2} measurement with
 a Impedance analyser
 b WF transfer function

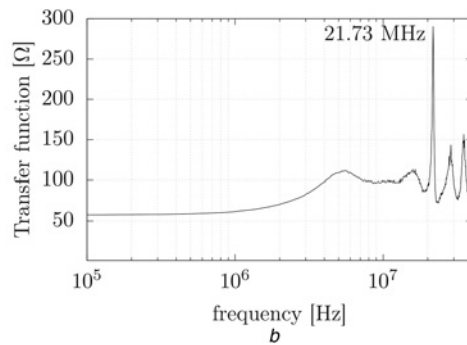
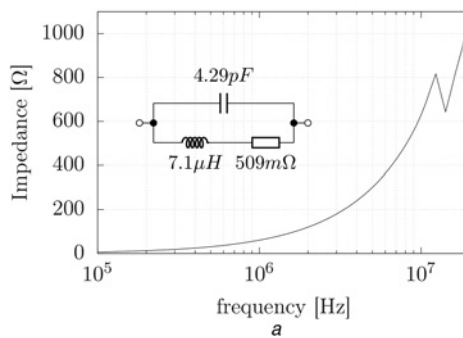


Fig. 10 C_{M3} measurement with
 a Impedance analyser
 b WF transfer function

frequencies $f_1 = 404$ kHz, $f_2 = 397$ kHz and $f_3 = 21.73$ MHz. It allows to calculate the capacitance $C_{M1} = 1.23$ nF, $C_{M2} = 1.27$ nF and $C_{M3} = 4.46$ pF. The capacitance of transformer are estimated

using formulas (7), (8) and (9): $C_1 = 4.46$ pF, $C_2 = 96.21$ pF and $C_{12} = 40.6$ pF. Results obtained using WF method are compared with measurements using impedance analyser (Table 4).

Table 4 Comparison of stray capacitances measured by impedance analyser C_{ia} and estimated by WF method C_{WF}

	C_{ia} [pF]	C_{WF} [pF]
C_{M1}	1198	1230
C_{M2}	1238	1270
C_{M3}	4.29	4.46
C_1	4.29	4.46
C_{12}	40	40
C_2	97.7	100.2

8 Conclusion

It has been developed a new estimation method of transformer parasitic capacitances. In this method, any physical or geometrical transformer data are required. The method is based on WF of transformer resonant frequencies in the selected three measurement setups. Thus, an influence of parasitic components in cables, supply and measurement connections has been limited. Application of the method allows to determine the transformer impedance in a high frequency range without need of specialised

measurement equipment such as impedance bridge or impedance analyser. Moreover, calibration procedure is not necessary.

9 References

- 1 Longtao, L., Lixin, W., Chao, L., *et al.*: 'A simulation of conducted EMI in flyback converters'. 2012 Seventh Int. Power Electronics and Motion Control Conf. (IPEMC), June 2012, vol. 3, pp. 1794–1798
- 2 Tarateeraseth, V., Maneenopphon, T., Khan-Ngern, W.: 'The comparison of EMI and electrical performances of high frequency transformer windings for SMPS applications'. Power Conversion Conference – Nagoya, 2007. PCC'07, April 2007, pp. 435–440
- 3 Ryu, S.-H., Lee, B.-K.: 'Highly accurate analysis method for llc dcdc converters with an improved transformer circuit model', *Electronics Letters*, 2015, **51**, (12), pp. 928–930
- 4 Wang, Q., An, Z., Zheng, Y., *et al.*: 'Parameter extraction of conducted electromagnetic interference prediction model and optimisation design for a DC-DC converter system', *IET Power Electron.*, 2013, **6**, (7), pp. 1449–1461
- 5 Yazdani, M., Filabadi, N., Faiz, J.: 'Conducted electromagnetic interference evaluation of forward converter with symmetric topology and passive filter', *IET Power Electron.*, 2014, **7**, (5), pp. 1113–1120
- 6 Biela, J., Kolar, J.: 'Using transformer parasitics for resonant converters; a review of the calculation of the stray capacitance of transformers', *IEEE Trans. Ind. Appl.*, 2008, **44**, (1), pp. 223–233
- 7 Xinkui, M., Wei, C.: 'More precise model for parasitic capacitances in high-frequency transformer'. Power Electronics Specialists Conf., 2002. pesc 02. 2002 IEEE 33rd Annual, 2002, vol. 2, pp. 1054–1057
- 8 Baktash, A., Vahedi, A.: 'Calculation of parasitic elements in toroidal core transformers', *Plasma Science, IEEE Transactions on*, 2014, **42**, (6), pp. 1690–1696
- 9 Saravi, S., Tahani, A., Zare, F., *et al.*: 'The effect of different winding techniques on the stray capacitances of high frequency transformers used in flyback converters'. Power and Energy Conference, 2008. PECon 2008. IEEE 2nd International, December 2008, pp. 1475–1478
- 10 Lu, H.-Y., Zhu, J.G., Hui, S.: 'Experimental determination of stray capacitances in high frequency transformers', *IEEE Trans. Power Electron.*, 2003, **18**, (5), pp. 1105–1112
- 11 Zhongyuan, Z., Fangcheng, L., Guishu, L.: 'A high-frequency circuit model of a potential transformer for the very fast transient simulation in GIS', *IEEE Trans. Power Deliv.*, 2008, **23**, (4), pp. 1995–1999
- 12 Pramanik, S., Satish, L.: 'Estimation of series capacitance for a three-phase transformer winding from its measured frequency response', *IEEE Trans. Power Deliv.*, 2013, **28**, (4), pp. 2437–2444
- 13 Abeywickrama, N., Serdyuk, Y., Gubanski, S.: 'High-frequency modeling of power transformers for use in frequency response analysis (FRA)', *IEEE Trans. Power Deliv.*, 2008, **23**, (4), pp. 2042–2049
- 14 Suwarno Donald, F.: 'Frequency response analysis (FRA) for diagnosis of power transformers'. 2010 Int. Conf. on Electrical Engineering/Electronics Computer Telecommunications and Information Technology (ECTI-CON), May 2010, pp. 112–116
- 15 Aguglia, D., Viarouge, P., Martins, C.: 'Frequency domain non-linear identification method for high voltage pulse transformers'. 2012 XXth International Conference on Electrical Machines (ICEM), September 2012, pp. 1977–1983
- 16 Neumayer, M., Bretterklieber, T., Zangl, H.: 'Bayesian estimation of electrical transformer parameters'. Proc. 2014 IEEE Int. Instrumentation and Measurement Technology Conf. (I2MTC), May 2014, pp. 514–518
- 17 Vaseghi, S.-V.: 'Advance digital signal processing and noise reduction' (John Wiley and Sons Ltd, 2000)
- 18 Musznicki, P., Schanen, J.-L., Granjon, P., *et al.*: 'The wiener filter applied to EMI decomposition', *IEEE Trans. Power Electron.*, 2008, **23**, (6), pp. 3088–3093
- 19 Yang, Y., Wang, Z.-J., Cai, X., *et al.*: 'Improved lumped parameter model for transformer fast transient simulations', *IET Electr. Power Appl.*, 2011, **5**, (6), pp. 479–485
- 20 Cogitore, B., Keradec, J., Barbaroux, J.: 'The two-winding transformer: an experimental method to obtain a wide frequency range equivalent circuit', *IEEE Trans. Instrum. Meas.*, 1994, **43**, (2), pp. 364–371
- 21 Schellmanns, A., Keradec, J.-P., Schanen, J.-L., *et al.*: 'Representing electrical behaviour of transformers by lumped element circuits: a global physical approach'. Conf. Record of the 1999 IEEE Industry Applications Conf., 1999. Thirty-Fourth IAS Annual Meeting. 1999, vol. 3, pp. 2100–2107